RSC Sustainability

ROYAL SOCIETY OF CHEMISTRY

PAPER

View Article Online
View Journal | View Issue

Check for updates

Cite this: *RSC Sustainability*, 2025, **3**, 3437

Green beginnings: creating an affordable advanced enquiry-based experimental nanochemistry learning module with catalytically active 'green' iron oxide nanoparticles (IONPs)†

Timothy Schwantes, Dylan Medina, Brittney Morgan and Abhinandan Banerjee *

In the following report, we disclose an affordable, scalable, and 'green' inaugural experiment for a nanochemistry and nanomaterials teaching laboratory course. Iron oxide NPs (IONPs) generated through co-precipitation is a well-known class of nanomaterials. They combine a relatively simple synthesis with an abundance of pedagogy-friendly functional properties such as energy band-gap, surface charge and capping ligand properties, size, morphology, crystal phase, and magnetic behaviour. Additionally, catalytic behaviour shown by IONPs in Fenton-type reactions provides us with an easy application suitable for the undergraduate laboratory. This month-long synthesis, purification, characterization, and application 'mini-project' is meant for inclusion in upper-division courses in inorganic chemistry or materials science. We believe that it sets students up for success in and outside a teaching laboratory and can be implemented in the first weeks of a course-based undergraduate research experience (CURE) as a way to acquaint students to the necessary skills to engage in authentic research. This project is also in close alignment with the United Nations sustainable development goals (SDG) numbers 4 (Quality Education for All) and 6 (Clean Water and Sanitation).

Received 7th February 2025
Accepted 4th May 2025

DOI: 10.1039/d5su00083a

rsc.li/rscsus

Open Access Article. Published on 06 2025. Downloaded on 05-12-2025 9:17:44.
This article is licensed under a Creative Commons Attribution-NonCommercial 3.0 Unported Licence.

Sustainability spotlight

Quality education, clean water and sanitation, and reduced inequalities are three key aspects of the United Nations Sustainable Development Goals (SDG 4, 6, and 10 respectively). This communication highlights a multiweek project using a green and affordable material – CTAB capped iron oxide nanoparticles (IONPs) – whose synthesis, characterization, and functional application in dye-contaminated water remediation expose students to a typical research workflow within a course-based laboratory environment. This experiment may be tuned to fit various time frames and resource availability scenarios, but the core synthesis of the IONPs and their application in the removal of methylene blue from water (the progress of which process may be followed using ultra-cheap visible spectrophotometers) constitute a robust, affordable, and sustainable experimental framework within which the scientists of tomorrow learn not only about chemical processes, but also about their application in solving real-world problems. Finally, in the context of an inaugural experiment for a nanochemistry teaching laboratory, this experiment provides students with a 'nano toolkit' of characterization techniques that they will revisit repeatedly during the course, thereby implementing scaffolded learning within a laboratory environment.

1 Introduction

The chemistry of nanomaterials permeates every aspect of our daily lives, such as health,[1] energy,[2] industrial production of chemicals and consumer goods,[3] and the environment,[4] often changing our lives enormously for the better, but sometimes bringing new concerns along with improvements.[5,6] In response to this development, many chemistry programs around the world have incorporated at least one nanochemistry course as a part of their undergraduate (UG) curriculum, especially for students seeking a specialized chemistry degree.[7,8] However, less frequently has a laboratory module – either standalone or conducted in parallel with lectures – been made available to these students.[9,10]

One of the major reasons behind this omission might be the cost associated with running such a laboratory course. Nanochemistry laboratories are often expensive to run, since the fundamental characterization protocols for nanomaterials, such as phase identification of inorganic nanoparticles using

Department of Chemistry, Colorado State University, Centre Mall, Fort Collins, CO, USA. E-mail: abhinandan.banerjee@colostate.edu; Tel: +1 970 491 2130

† Electronic supplementary information (ESI) available: (a) Plan of work; (b) sample pre-lab questions; (c) instructions to students for the synthesis of IONPs and their catalytic application in methylene blue degradation; (d) notes supplied to students for the processing of UV-Visible data to obtain a Tauc plot for the IONPs; (e) IR peak assignment; (f) compendium of discussion type questions including the catalytic mechanism. See DOI: https://doi.org/10.1039/d5su00083a

© 2025 The Author(s). Published by the Royal Society of Chemistry

Open Access Article. Published on 06 2025. Downloaded on 05-12-2025 9:17:44.
This article is licensed under a Creative Commons Attribution-NonCommercial 3.0 Unported Licence.

Table 1 Data processing and analysis techniques associated with this experiment

Nanomaterial property	Measurement technique	Data processing skill	Software
Band gap	UV-vis spectroscopy	Tauc plot	OriginLab™
Hydrodynamic radius	Dynamic light scattering	Data extraction and plotting	OriginLab™
Size and morphology	Scanning electron microscopy	Size evaluation from micrograph, size distribution profile	FiJi
Phase identification	PXRD	Phase matching with standard powder patterns	Mercury™
Magnetic moment and T_b	SQUID magnetometry	Data extraction and plotting	OriginLab™
Surface functionality identification	IR spectroscopy	Peak picking and assignments	OriginLab™

powder X-ray diffraction (PXRD) or nanomaterial imaging using scanning or transmission electron microscopy (SEM, TEM) require access to sophisticated equipment, typically unavailable in UG teaching laboratories.‡ However, this omission detracts from the learning experience. When it comes to the chemistry of functional nanomaterials, passive observation is a poor replacement for active enquiry-based education.[11] Moreover, the problem of instrument availability is often circumvented in the larger universities by collaboration, either with research groups having access to the necessary instruments; or better yet, with a central research instrumentation facility affiliated with the university. In our opinion, it is not imperative for the UG students to operate these instruments; instead, the focus should be on the processing and analysis of the data harvested from the instruments (Table 1 mentions the relevant examples from this specific experiment). This is not a trivial exercise and often needs specialized software, for which students need proper training. Fortunately, many of these tools are available as freeware,[12] or have free and open-source (FOSS) alternatives, such as FiJi. We contend that creating, curating, and maintaining an UG nanochemistry teaching laboratory is a highly productive and rewarding exercise leading to immense benefit for the chemistry major of the 21st century. At Colorado State University, Fort Collins, we offer a chemistry of nanomaterials laboratory for third- and fourth-year UG students. While not mandatory, it is strongly recommended that students enrolling in the nanomaterials theory course take this laboratory class as well. It is presently in its second iteration and we expect to offer the course every year in tandem with the relevant lecture module. Future iterations of the course will move towards a course-based undergraduate research experience (CURE) model, implementing the experiment described herein during the first few weeks to expose student to standard laboratory procedures and skills needed to test their own independent hypotheses.

Extensive literature highlights the benefits of undergraduate research in enhancing academic achievement and advancing career success.[13–15] CUREs offer similar benefits of independent research, such as improved retention of students and more equitable learning outcomes, while addressing barriers to participating in UG research experiences.[16] Expanding access to these research experiences, which can be accomplished by implementing the CURE model, is imperative as student demand for such experiences grows exponentially, while the number of faculty members available to provide them remains relatively constant.[17,18] However, the field of inorganic chemistry is largely underrepresented among those courses that have implemented the CURE model[19] and there have been calls for quality, relevant curricular materials developed for inorganic chemistry laboratories in general.[20] There has been an increase in focus on transition metal-related topics, including functional inorganic materials and nanoscience, in foundational inorganic chemistry lecture courses.[21] Consequently, laboratory courses should be designed to align with these prominent topics and emerging interests in the field as the effectiveness of any CURE relies on the relevance of the work and the opportunity for students to build upon and contribute to current scientific consensus in a broader scope outside of the classroom.[19]

Green chemistry and its implementation across various sectors continues to be explored as a pathway to sustain innovation and societal growth;[22] for this reason the interface between green chemistry and nanochemistry should be explored during the course of a chemistry degree. Although experiments typically associated with a teaching laboratory exploring the chemistry of nanomaterials can be green, they very often are not, owing to the use of highly toxic precursors (synthesis of cadmium selenide quantum dots is a representative example),[23] energy-intensive techniques (such as hot injections and solvothermal syntheses of metal and metal oxide nanostructures[24]), or the use of specific high-boiling solvents and additives (such as etchants) which are essential for controlling NP shapes, sizes, surface functionalities, and other properties.[25] In research facilities, this is often mitigated or offset by microscale synthesis of nanomaterials, but it is unreasonable to expect a student beginning to learn about the intricacies associated with the synthesis of these nanostructured morsels of matter to simultaneously perform those steps at the microscale. For our very first enquiry-based learning project in the nanochemistry teaching laboratory, therefore, we designed an experiment which mitigated the aforementioned concerns by being centred around one of the greenest materials known to the nanomaterials community: nanostructured iron oxide,[26–28] capped with CTAB (cetyltrimethylammonium bromide), a generally-recognized-as-safe (GRAS) surfactant.[29,30] Alongside the easy synthesis of IONPs (*vide infra*), this experiment provides students with an opportunity to be trained in multiple fundamental techniques used in the functional characterization of inorganic nanomaterials, such as transition metal chalcogenides. Iron oxide nanoparticles (IONPs) are

‡ From https://www.nanoimages.com/tabletop-sem-products/, accessed on 26 Dec 2024: Tabletop SEM models range in price from 60 000 to 120 000 USD, while traditional tungsten-source SEMs range in price from 120 000 to 250 000 USD.

© 2025 The Author(s). Published by the Royal Society of Chemistry

Open Access Article. Published on 06 2025. Downloaded on 05-12-2025 9:17:44.
This article is licensed under a Creative Commons Attribution-NonCommercial 3.0 Unported Licence.

known for their high magnetic susceptibility, bio-compatibility, inherent 'greenness', and potential for easy surface modification, making them an excellent candidate for our introductory nanochemistry lab.[31] IONPs have been used in sensors, as vectors for targeted drug delivery, for magnetic hyperthermia, as magnetic resonance imaging (MRI) contrast agents,[32–35] for catalysis,[36–38] in environmental remediation[39] and in spintronics.[40] Owing to their multiplicity of applications, many reviews have been devoted to these unique materials. Several methodologies, including physical,[41,42] chemical,[43,44] and biological,[45] have been used to generate IONPs; among these, the co-precipitation method stands out as the most popular wet-chemical approach to synthesize spherical IONPs, with very basic equipment, albeit with limited control over NP size and morphology.[46] The IONPs are readily separable from the reaction mixture by the use of a strong magnet, making the washing step quick and easy. The IONPs are then subjected to our arsenal of characterization techniques to examine their properties, including morphology, dimensions, surface composition, semiconductor band gap, magnetic susceptibility, and phase composition.

The treasury of data that the students obtain from this multi-week characterization session provides them with preliminary exercises in data collection, processing, analysis, and interpretation.[24] The key idea behind this experiment is to train students in the basic techniques of inorganic nanoparticle characterization using a material they themselves have synthesized, which is preferable to the use of commercial and/or presynthesized samples. It is our contention, borne out by observation, that students are more interested in examining the materials they have created on their own. This multi-week laboratory experiment sets the stage perfectly for a series of subsequent, more specialized experiments where the students will use one or more of the techniques in which they have been trained during the course of this inaugural experiment to explore their own hypotheses. We also note in passing that this 'mini-project' aligns with UN SDG numbers 4 (providing quality education and hands-on laboratory training, especially to our future scientists-in-training) and 6 (ensuring availability and sustainable management of water and sanitation through effective wastewater remediation).[47]

2 Materials and methods

2.1 Student cohort and learning objectives

The students enrolled in this laboratory course were juniors and seniors (third- and fourth-year students) majoring in chemistry at Colorado State University (Fort Collins); they had, in the past, successfully completed the introductory inorganic chemistry module, including a laboratory component and associated laboratory safety training (including the study of MSDS for hazard warnings). Under the supervision of the graduate teaching assistant (DM), the students worked individually to complete this experiment over the course of five 3 h laboratory sessions, meeting once a week for a month. The experiment was planned as an exercise in enquiry-based learning, encouraging the students to discover the answers to a series of scientific questions each day even as they expanded their technical capabilities through exposure to a series of characterization techniques they were to encounter regularly in subsequent experiments. These learning objectives can be summarized as follows:

- Preliminary training in NP synthesis through co-precipitation under an inert atmosphere.
- Training in commonly used chemistry sample preparation and isolation protocols such as centrifugation, drop-casting, decantation, magnetic separation, and others.
- UV-visible and IR spectroscopy including data interpretation through comparison with literature examples (*n.b.* – data collected by students).
- Training in the use of a DLS instrument for NP size and surface charge determination. (*n.b.* – data collected by students).
- Data processing and interpretation for assessing the characteristics of the synthesized nanoparticles: PXRD, SEM, and magnetometry.
- Developing data visualization and scientific communication skills.

For the techniques where we were unable to let the students use the instruments independently (SEM, PXRD, SQUID magnetometry), they were given a tour of the instrument and witnessed the sample loading and/or imaging steps. For UV-Vis, IR, and DLS, students were instructed in the principles behind the technique and performed the protocol themselves while closely monitored by ARB, TS, or DM.

2.2 Materials

$FeCl_2$, $FeCl_3$, concentrated HCl, concentrated NH_4OH, NaOH pellets, and solid CTAB were purchased from Millipore Sigma and used without any purification. DI water was used throughout the experiment. Nitrogen gas (technical grade) was purchased from AirGas. Methylene blue powder was obtained from HiMedia (Amazon, HiMedia GRM956-100G Methylene Blue) and used as received.

2.3 Preparation of stock solutions for the IONP synthesis

We prepared the following solutions for the students: 2 (M) $FeCl_2$ in 2 (M) HCl; 1 (M) $FeCl_3$ in 2 (M) HCl; 5 m (M) aqueous CTAB solution; 0.7 (M) NH_4OH in water. Acids and bases were stored separately, in different fume hoods. Appropriately labeled graduated cylinders were placed next to the stock solutions to avoid any confusion during transfer.

2.4 Synthesis of the IONPs

Step-by-step instructions for the synthesis supplied to the students may be found in the ESI.† In summary, 1 mL of the stock solution containing 2 (M) $FeCl_2$ in 2 (M) HCl and 4 mL of the 1 (M) $FeCl_3$ solution in 2 (M) HCl were thoroughly mixed in a two-neck round bottom flask charged with a magnetic stir bar, to which 10 mL of the CTAB solution was added. This mixture was heated to 70 °C under a dynamic flow of nitrogen with continuous stirring (Fig. 1). After 30 minutes, a 25 mL burette containing the base was clamped onto the reaction flask and,

Open Access Article. Published on 06 2025. Downloaded on 05-12-2025 9:17:44.
This article is licensed under a Creative Commons Attribution-NonCommercial 3.0 Unported Licence.

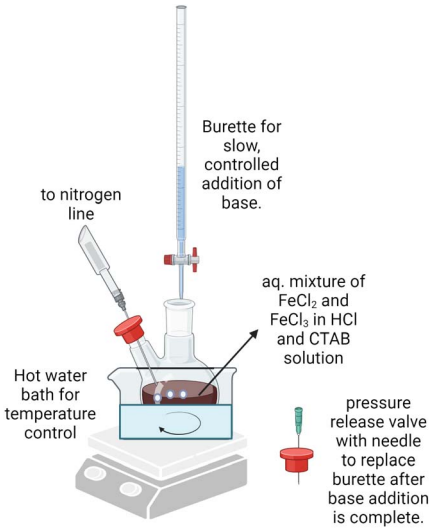

Fig. 1 Experimental set-up for the synthesis of IONP@CTAB by students.

while stirring, the burette stopcock was slowly opened to add the base dropwise at a rate of no more than 1 mL every 10 s to the main reaction mixture. Once half of the burette was emptied, the pH of the reaction mixture was tested with an indicator strip. If pH was less than 10, addition of base was resumed; if the entire burette was emptied, then it was refilled using a funnel. Typically, this is needed only once. Upon reaching the desired pH (~10–11), the base addition was stopped and the flask was sealed with a septum equipped with a needle vent. The heating, the nitrogen flow, and the stirring were continued for another 15 min. Then, another 10 mL of the CTAB solution was added and the heating and nitrogen flow stopped. The IONPs were allowed to stagnate and settle for 5–10 minutes; they accumulated at the bottom of the vial in a distinct layer. The liquid on the top was decanted, and the IONPs were magnetically separated from the reaction mixture. They were washed with the CTAB solution twice, recovered magnetically each time, and finally stored in a 50 mL centrifuge tube at 4 °C. Bare IONPs without the CTAB coating were also synthesized for comparison; this can be done by the students during this synthesis (see ESI† for details) or prepared ahead of time by the instructor, and supplied to the students. A brief description of the mechanism of formation of IONPs under these conditions can be found in the ESI.†

2.5 Sample preparation for characterization techniques

The students were encouraged to observe and participate in sample preparation for the various characterization techniques. The students themselves prepared the samples for UV-visible spectroscopy, IR spectroscopy, DLS, and SEM. For SQUID magnetometry and PXRD, only one sample could be analyzed; therefore, the students observed the sample preparation as performed by the TA.

2.5.1 UV-visible spectroscopy. For recording the optical spectrum of the precursor, the mixture of iron (II) and (III) chlorides in aq. HCl was diluted with DI water; then, their spectrum was recorded using a quartz cuvette in a Vernier GoDirect spectrophotometer. DI water was used as the background. 0.1 mL of CTAB-capped IONP dispersion was added to 30 mL of DI water, sonicated for 15 min, and 1 mL of this was added to a quartz cuvette containing 2.5 mL of DI water, thoroughly mixed, and the spectrum was recorded. The students were given instructions on the conversion of the UV-Vis data for the CTAB-capped IONPs to a representative Tauc plot for the estimation of the band-gap of IONP@CTAB (ESI†).

2.5.2 ATR-IR spectroscopy. The students recorded ATR-IR spectra for CTAB, bare IONPs, and IONP@CTAB on a Nicolet Summit portable IR system. The number of scans per sample was fixed at 32, and the resolution was set at 8 cm^{-1}. The students were encouraged to re-plot their data and identify/highlight chemically relevant peaks for each sample.

2.5.3 Dynamic light scattering. In order to determine the average dimensions of the IONPs, dynamic light scattering (DLS), also known as photon correlation spectroscopy, was applied. This technique measured hydrodynamic diameters of the IONP@CTAB, as well as the polydispersity index (PDI). Diluted samples (50- to 100-fold dilutions) were used to avoid multiple scattering, and the samples were sonicated in a commercial ultrasonic bath (US Solid) for 10 minutes prior to measurements. Aggregates were eliminated by filtration through a 0.22 μm PTFE syringe filter. The measurements were conducted using the Litesizer 500 (Anton Paar) and the particle dimensions were calculated from the autocorrelation function of the intensity of light scattered from the particles. The software used was Anton Paar Kalliope, supplied by the manufacturer. Disposable poly(styrene) cuvettes were used for sample measurements.

The rate of droplet movement under the influence of an external oscillating electrical field with a voltage of 200 V (electrophoretic mobility) was also measured with the Litesizer in folded capillary omega cells obtained from Anton Paar (225288). The measured electrophoretic mobilities were converted to ζ-potentials by the instrument software using Henry's equation:

$$U_e = \frac{2\varepsilon\zeta}{3\eta} \cdot f_{ak} \quad (1)$$

where U_e is the electrophoretic mobility, ε is the dielectric constant, ζ is the zeta potential, η is the viscosity of the dispersant, and f_{ak} is the Henry function. The Smoluchowski approximation, $f_{ak} = 1.5$, was used for high ionic strength media, given that water was the bulk phase in all the measured systems. It is to be noted that the DLS measurements were performed by the students themselves with some guidance from a TA who was previously given extensive training on the instrument.

2.5.4 Scanning electron microscopy. IONP@CTAB samples were diluted ten-fold in water, and sonicated in a commercial ultrasonic bath (US Solid) for 10 minutes. 50 μL of the diluted IONP@CTAB sample was drop-cast directly on a SEM sample stub, and allowed to dry for a week. The following week, a two-hour session was dedicated to examining the student samples under a JEOL JSM-IT800(HL) field emission SEM and recording

© 2025 The Author(s). Published by the Royal Society of Chemistry

Open Access Article. Published on 06 2025. Downloaded on 05-12-2025 9:17:44.
This article is licensed under a Creative Commons Attribution-NonCommercial 3.0 Unported Licence.

micrographs. This part of the experiment was performed by ARB, with the students and the TA present in the room for the duration of the experiment. The students were previously trained on extracting average particle sizes and particle size distributions from the images using FiJi.

2.5.5 Powder X-ray diffraction. A slurry of the CTAB-capped IONPs was drop-cast on a zero background holder and allowed to dry overnight. The sample was then handed over to the XRD scientist at CSU's central instrumentation facility, who recorded a diffractogram of the sample on a Bruker D8 Discover DaVinci with Cu-K_α X-ray source. The data was communicated directly to the students, who were instructed to plot a diffractogram from the experimental data. The students were also trained on obtaining .cif files for the four probable phases present within their system (magnetite, maghemite, hematite, and goethite) from the open crystallographic database. They then opened the .cif files using Mercury™, a free crystal structure visualization tool developed by the Cambridge Crystallographic Data Centre.[48] The students obtained the powder diffraction pattern for each 'standard' phase of interest, and plotted the relevant diffractograms directly under the experimental diffractogram for phase identification through visual inspection.

2.5.6 SQUID magnetometry. ≤5 mg of the IONP@CTAB was carefully weighed out and introduced into a sample holder for Quantum Design MPMS3 SQUID. The exact weight of the sample was recorded, correct to the nearest 0.1 mg. After being properly centred, the magnetic moment of the sample was measured as a function of the applied magnetic field at 2 K and 300 K. Relevant sequence files for the MPMS are available upon request.

2.6 IONP@CTAB catalyzed degradation of methylene blue in simulated wastewater

This part of the experiment was performed in groups of two. One student added 5 mL of 30% H_2O_2 from the refrigerator to 95 mL of 0.16 mM methylene blue solution in a 200 mL beaker. To this was added 2.5 (M) NaOH solution drop-wise to raise the pH of the system approximately to 11. Finally, the student added 25 mg of the dry IONP@CTABto the mixture, and stirred it vigorously for 30 seconds with a glass stir rod. After the IONPs were added and stirred, the deep azure colour of the mixture visibly lightened. After this initial stirring, the beaker was allowed to sit uninterrupted as the reaction progressed. The colour of the mixture began to lighten visibly over time. The other student in the group withdrew aliquots from the reaction beaker every fifteen minutes to record the UV-visible spectra. It may be noted that the reaction continues in the cuvette after measurements, and an 'in-cuvette' reaction may be an alternative experimental setup to follow the IONP@CTAB catalyzed oxidative degradation of methylene blue in aqueous solution.

While we did encourage the students to magnetically recover the IONP@CTAB from their reaction mixtures after complete bleaching of the blue colour, we did not attempt to use the recovered material in a second catalytic cycle to illustrate the recyclability typically associated with IONP catalysts.

3 Results and discussions

It is to be noted here that the 'discussion' for each characterization technique should be driven by the students in consultation with the TA. The students should already be proficient in (or be given instructions on) using a scientific search engine such as SciFinder or Google Scholar to access publications that have previously characterized IONPs. They should then extract the relevant results from these reports and compare those with the data they have recorded in class. This comparison was assigned as a continuing 'at home' assignment for the duration of the project.

3.1 UV-visible spectra and Tauc plot

Fig. 2 represents the UV-visible spectra of the iron precursors in acidic solution, as well as that of the IONP@CTAB. For the mixed iron chlorides dissolved in 2 (M) HCl, the spectrum exhibits a single peak around 300 nm, typically associated in the literature with various $[FeCl_x]^{y+}$ species.[37] These bands were absent in the IONP@CTAB samples; instead, a shoulder appeared at higher wavelengths, indicating conversion of the iron chlorides to IONPs.

The students converted the UV-visible spectrum of the IONP@CTAB to a Tauc plot by using the Tauc equation, represented below. This plot is used extensively for easy determination of the approximate optical band-gap of semiconductors through simple extrapolation.[49] Details for the calculations may be found in the ESI.†

$$(\alpha h\nu)^n = K(h\nu - E_g) \quad (2)$$

The band gap energy of IONP@CTAB is determined from the Tauc plot, wherein $(\alpha h\nu)^n$ is plotted as a function of $h\nu$, followed by taking the extrapolation in the linear area across the energy axis in the corresponding graph [Fig. 2(b)]. The students obtained a value of E_g between 2.5 and 2.8, which is on the higher side of optical band gaps recorded for IONPs.[50] The instructors can tell students at this point that this extrapolation strategy, despite widespread use owing to its simplicity, has several drawbacks, and many complex modifications have been suggested for more accurate determination of the optical band-gap of NPs from their spectroscopic data.[51]

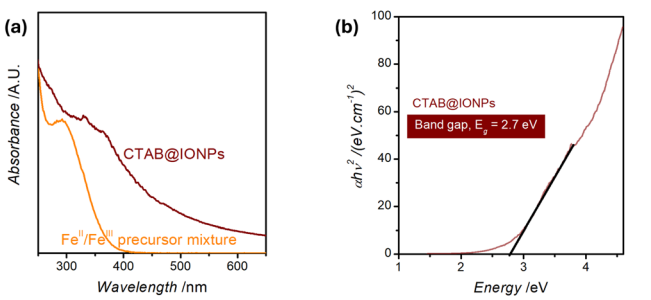

Fig. 2 (a) UV-visible spectra of the precursor mixture and the IONP@CTAB. (b) Tauc plot for IONP@CTAB with extrapolated line showing band gap energy calculation.

Open Access Article. Published on 06 2025. Downloaded on 05-12-2025 9:17:44.
This article is licensed under a Creative Commons Attribution-NonCommercial 3.0 Unported Licence.

3.2 IR spectroscopy

IR spectroscopy plays a vital role in determining the surface composition of nanoparticulate matter, which in turn has a profound effect on their functional properties, such as solubility and catalytic behaviour.[52] It is important, therefore, for students to identify IR bands which may be attributed to the composition of the NPs themselves (for instance, in Fig. 3, the band at *ca.* 560 cm^{-1} may be attributed to Fe–O–Fe stretching vibrations originating from the iron oxide core) *vis-a-vis* the bands originating from the capping ligand on the NP surface (here CTAB, showing, among others, a prominent N–CH_3 asymmetric stretching band around 1480 cm^{-1}).[53] A sample peak attribution list for IONP@CTAB may be found in the ESI (Section S6 and Table S1†). We note at this point that scavenging the relevant nanochemistry literature, as well as standard introductory spectroscopy texts, for assigning observed IR bands was part of the designated 'homework' for the second week of the experiment (Table 2). The small difference for asymmetric and symmetric C–H scissoring vibrations of the N–CH_3 moiety between pure CTAB molecules and IONP@CTAB was pointed out to the students as an evidence of CTAB adsorbing on the IONP surface through its headgroup. The characteristic [C–H···metal] vibration band was not observed, indicating the absence of C–H binding to the NP surface.[54] This kind of guided interpretation encourages students to think beyond rote peak assignment while handling spectral data.

3.3 Dynamic light scattering

Fig. 4 represents the information the students obtained about their IONP@CTAB dispersed in water, using DLS as a measurement technique. The average hydrodynamic diameter of the IONP@CTAB was found to be 167 ± 3 nm, with an average polydispersity index of 0.14. As expected, the IONP@CTAB demonstrated a positive surface zeta potential, with an average value of 31.7 ± 0.6 mV. This value was in agreement with previously recorded zeta potential values for IONP@CTAB in the literature.[55] The students were reminded at this point that a numerical value of the zeta potential ≥30 mV indicated a definite contribution of electrostatics towards NP–NP repulsion and consequent stabilization of the dispersion.[55]

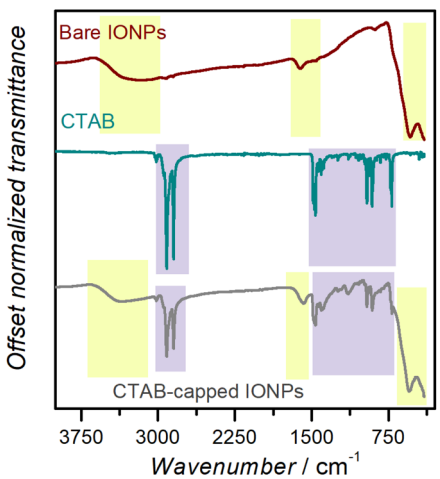

Fig. 3 IR bands for bare IONPs, CTAB, and IONP@CTAB. The boxes in lavender contain IR bands which may be attributed to CTAB, while the ones in lime originate from the IONPs.

Table 2 Homework assignments associated with this project

Week	Homework assignments
1	UV-vis data plotting Tauc plot and band-gap determination
2	DLS data plotting IR data plotting, peak assignment, literature comparison
3	Particle size distribution from SEM PXRD data plotting, phase identification
4	Magnetometric data plotting [$M(H)$ curves] Catalytic data processing
5 (final)	Report in communication format

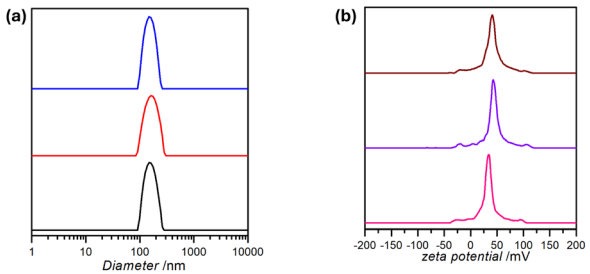

Fig. 4 (a) Size distribution profile, and (b) zeta potential measurement for the IONP@CTAB.

3.4 Scanning electron microscopy

The students were given a brief introduction to electron microscopy before accompanying ARB and DM for their first 'live' SEM experience. Students were encouraged to make notes and ask questions during the measurement process, with ARB performing the imaging and DM providing explanations. The students were supplied with the images of their samples, and in consultation with them, we selected the best IONP@CTAB sample in anticipation of image processing and measurement training using FiJi. FiJi is a free image processing package which bundles many plugins, facilitating scientific image analysis (including measurements in the presence of a scale-bar).[56] The students downloaded FiJi on their personal computers and were trained on setting the scale bar and measuring individual NP diameters. These measurements were then exported to OriginLab for plotting the particle size distribution profile. Fig. 5 shows two representative SEM images. The students each measured at least 100 IONP@CTAB diameters and pooled the data for the statistical plot [Fig. 5(c)].

3.5 PXRD and phase identification of the IONP@CTAB

PXRD and phase identification are typically performed on nanomaterials such as iron oxides, which have multiple phases, with hematite, maghemite, and magnetite being the most common ones.[57] IONPs exhibit phase-dependent physical and

© 2025 The Author(s). Published by the Royal Society of Chemistry

Open Access Article. Published on 06 2025. Downloaded on 05-12-2025 9:17:44.
This article is licensed under a Creative Commons Attribution-NonCommercial 3.0 Unported Licence.

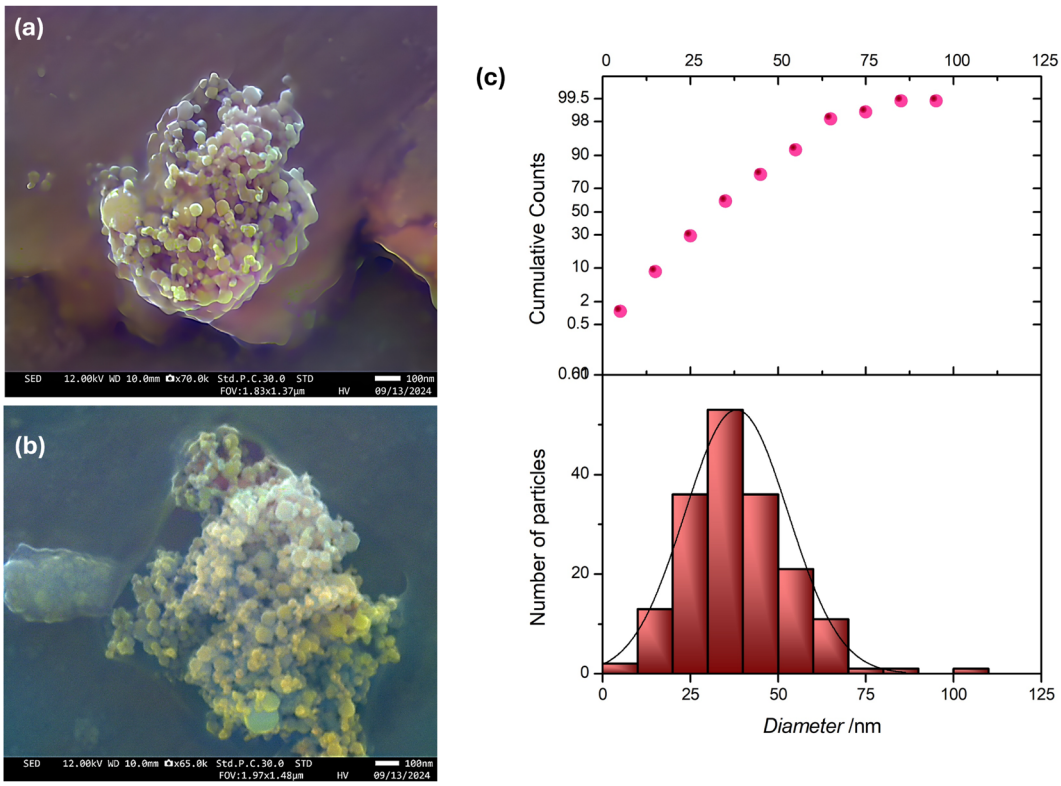

Fig. 5 (a and b) SEM secondary electrons images of two student samples, colorized through the use of AI (https://deepai.org/machine-learning-model/colorizer); (c) particle size frequency distribution profile and probability from manual measuring of at least 200 spherical IONP@CTAB from the images.

chemical characteristics such as reactivity, electrical conductivity, optical behaviour, and more.[58] With the advent of robust benchtop PXRD systems§ having relatively simple usage protocols, advanced teaching laboratories often include phase identification as a technique in which students are trained. The International Centre for Diffraction Data (ICDD) maintains a database of powder diffraction patterns, the Powder Diffraction File (PDF), including the *d*-spacings, which are related to angle of diffraction, and relative intensities of observable diffraction peaks.[59] In experimental research facilities, this database is used in tandem with a diffractometer for immediate phase identification. However, licensing costs for these databases often limit their availability to a few work-stations, usually connected to the diffractometer and therefore in perpetual use.¶ For materials whose phase compositions are limited to a few likely candidates, an excellent alternative to ICDD is the Crystallography Open Database (COD). COD is an open-access database of crystal structures with over 520 000 structures of small molecules and small to medium-sized unit cell crystals.[60] The crystallographic information files (.cif files) as defined by the International Union of Crystallography may be downloaded from this database, and opened with Mercury™ (*vide supra*). The standard powder patterns obtained for the standard phases may then be plotted directly underneath the experimental diffractogram, and the patterns matched through visual inspection. We initially supplied three .cif files to the students, corresponding to hematite, magnetite, and goethite; the data extraction, plotting, and visual phase matching of the powder pattern were carried out by the students under the supervision of the TA. However, upon recording an extended PXRD for this sample *post facto*, we did notice a very small peak at $2\theta \sim 18$ °C, which may indicate the presence of small amounts of maghemite (γ-Fe_2O_3). Hematite (α-Fe_2O_3), which is formed by the oxidation of magnetite at high temperatures, is less likely to be present in the IONP@CTAB. This is in accordance with the conclusions reached by LaGrow *et al.*, who used transmission electron microscopy, electron diffraction and room temperature ^{57}Fe Mössbauer spectroscopy to identify a distinct transition from an amorphous ferrihydrite phase to a mixture of magnetite–maghemite upon synthesis of IONPs through co-precipitation.[46] Fig. 6 depicts a model 'comparison' diffractogram; it is evident that magnetite (Fe_3O_4) is the best fit for the experimental diffractogram.

3.6 Magnetometry of the IONP@CTAB

IONPs are uniquely known for their magnetic properties, which make them useful in applications as divergent as T_2 MRI imaging and spintronics.[32,34] An advanced laboratory

§ See, for instance, the Proto AXRD, the Rigaku MiniFlex, the Brucker D6 Phaser, and others.

¶ Additional details concerning ICDD license types and prices may be obtained from https://www.icdd.com/licensing-process/.

Open Access Article. Published on 06 2025. Downloaded on 05-12-2025 9:17:44.
This article is licensed under a Creative Commons Attribution-NonCommercial 3.0 Unported Licence.

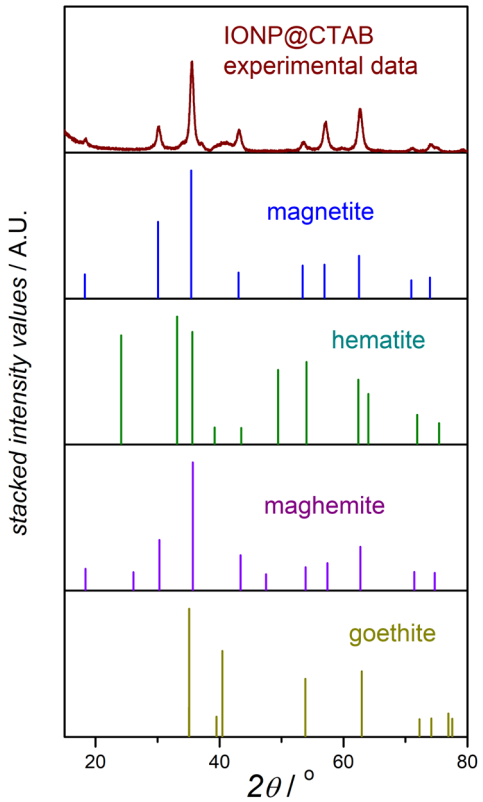

Fig. 6 Diffractogram: prepared sample (curve) and standard phases (matchstick plots) for matching through visual inspection by students.

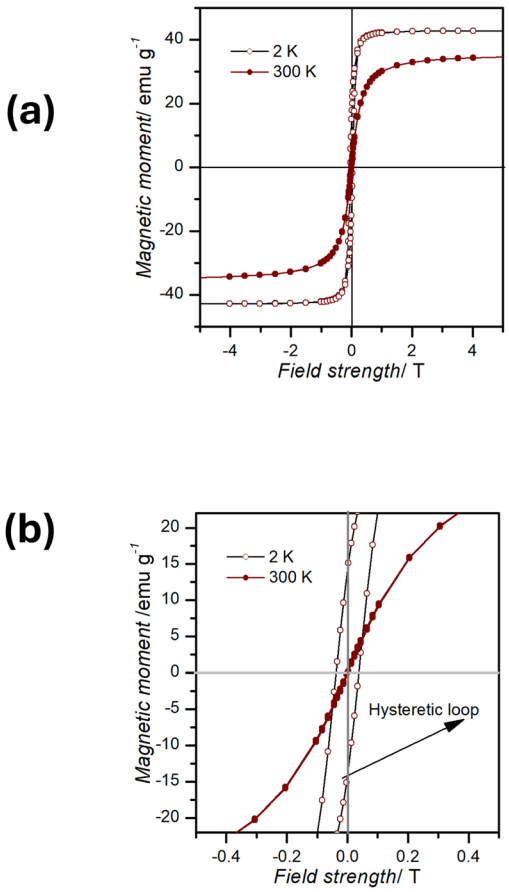

Fig. 7 (a) Measured magnetization *versus* field strength curves for IONP@CTAB; (b) shows a close-up of (a) at lower values of the applied magnetic field to represent the hysteresis shown by IONPs at 2 K but not at room temperature (~300 K).

experiment dealing with IONPs, therefore, should ideally quantify the magnetism of IONP@CTAB rather than simply demonstrate that the IONPs are attracted to magnets.[24] For this purpose, a VSM or a SQUID is ideal, especially one that allows the instructor to demonstrate to students that temperature plays a very important role in determining the magnetic behaviour of IONPs.

The following concepts were explained to the students to help them interpret the magnetic data:

• Powdered IONP@CTAB were used for the measurement. Thus, the measured magnetic properties represented the average values for an ensemble of randomly oriented nanoparticles.

• In the $M(H)$ curves, hysteresis was observed at 2 K, which is characteristic of ferromagnetic behaviour, while anhysteretic loops were recorded at room temperature.[32]

• Comparison of the recorded M_s values (emu g^{-1}) for the IONP@CTAB: bulk magnetite – 90; IONP@CTAB at 2 K – 42; IONP@CTAB at room temperature – 31. The students were made aware of the impacts of NP size and diamagnetic coating mass fraction on the M_s values of coated oxide nanoparticles.[61]

Finally, the students searched the literature to determine that our measured M_s values for the IONP@CTAB matched well with those recorded in other studies,[32] with slightly lower values of M which could be attributed to various factors. Of these, the easiest to explain is the diamagnetism of the CTAB shell capping the magnetic NPs; we do not account for the mass% of this shell when we record the mass of the NP sample inserted into the SQUID magnetometer (Fig. 7).

3.7 IONP@CTAB catalyzed methylene blue degradation using 'green' reagents

We selected the IONP-catalyzed degradation of methylthioninium chloride, also called methylene blue, a heterocyclic dye often found in industrial wastewater, in the presence of H_2O_2, as our trial reaction. This is an example of what is broadly classified as 'Fenton chemistry'.[62] While methylene blue has been used in healthcare, an excess of it can cause respiratory distress, abdominal disorders, blindness, digestive and mental disorders, and more. It can also irritate the skin and eyes, and cause nausea, vomiting, and diarrhea if ingested.[63] The removal of methylene blue from wastewater has therefore been studied extensively in a research context (*vide infra*, Table 3).

We note that there are three distinct benefits associated with this selection of a trial catalytic reaction:

(1) Hydrogen peroxide is an established 'green' oxidant since it converts to water – benign byproduct – upon decomposition, releasing nascent oxygen which behaves as a powerful oxidizer.[72]

© 2025 The Author(s). Published by the Royal Society of Chemistry

Open Access Article. Published on 06 2025. Downloaded on 05-12-2025 9:17:44.
This article is licensed under a Creative Commons Attribution-NonCommercial 3.0 Unported Licence.

Table 3 Selected examples of methylene blue degradation in water using catalytic iron-based nanomaterials

Iron-based NP catalyst	Rate constant (min^{-1})	Additive	Degradation time (% in min)	Reference
Biosynthesized α-Fe_2O_3 NP	0.0108	UV light	78% in 120 min	64
Yeast-supported nZVI[a]	0.0149	H_2O_2	91.9% in 600 min	62
PB-IONP[b]	N/A	H_2O_2	100% in 120 min	65
Rust	0.099	Ambient light	95% in 40 min	66
Fe_3O_4 nanorods	0.096	UV light	99.8% in 30 min	67
nZVI[a]	0.0141	H_2O_2	93% in 260 min	68
Fe_3O_4-GO[c]	N/A	Ambient light	75% in 75 min	69
Fe_3O_4 NPs	0.013	15 W white LED + H_2O_2	93.4% in 210 min	70
Mixed iron oxides/activated C	N/A	H_2O_2	70% in 180 min	71
CTAB-IONPs	0.025	H_2O_2	≥90% in 90 min	This work

[a] nZVI: nano zero-valent iron particles. [b] PB-IONP: Prussian-blue-modified iron oxide nanoparticles. [c] Fe_3O_4-GO: Magnetite-graphene oxide composites.

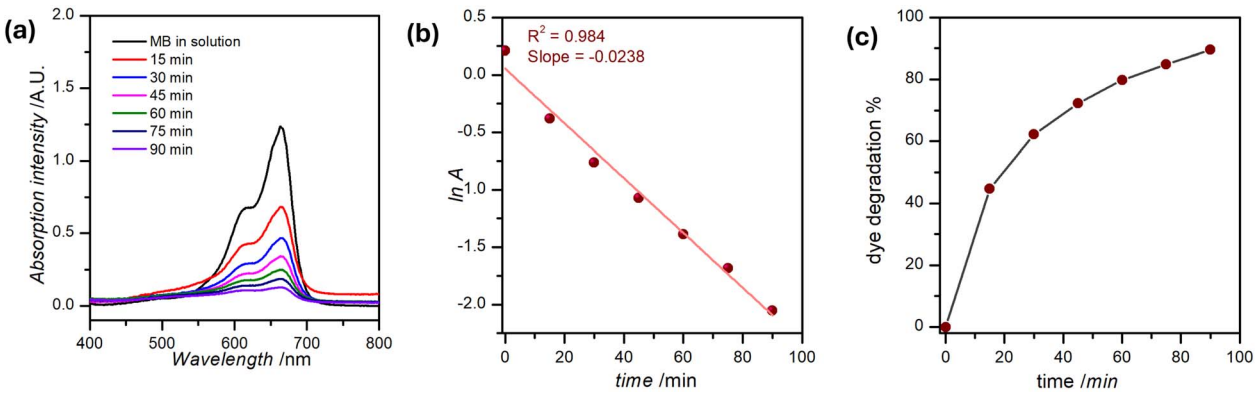

Fig. 8 (a) Methylene blue absorption at λ_{max} (~660 nm) reduces over time as the dye degrades; (b) the pseudo-first-order rate constant for this reaction may be estimated from the corresponding plot of ln *A* as a function of time; (c) percent dye degradation plotted as a function of time.

(2) IONPs are one of the most environmentally friendly and safe catalysts for peroxide-mediated oxidation of chemicals such as drugs, dyes, and other contaminants in matrices such as wastewater.

(3) The progress of the reaction can be followed and quantified spectrophotometrically, without the need for gas or liquid chromatography.

We know from literature that the reaction rates for iron oxide catalyzed degradation of many dyes in the presence of H_2O_2 depend profoundly on pH.[70] We selected a highly alkaline pH (10–11) for this reaction, to ensure completion of the reaction within the class time limits. We note here that methylene blue is a cationic thiazine dye. At high pH values, negatively charged ions, especially hydroxyl (OH^-), accumulate on the surfaces of IONP@CTAB, where the actual degradation of the dye occurs after the dye is sorbed onto the NP surfaces.[64] From Fig. 5, we note that *ca.* 90% of the methylene blue has been decolourized in less than 2 hours. This is broadly in agreement with studies that have reported a degradation of more than 95% for methylene blue at basic pH values within an hour or less.

We did not have the time or the opportunity to survey Fenton and Fenton-like chemistry with the students, but they were given a general picture of the reactions happening at the molecular level which lead to the decolourization of the dye in aqueous solution.[73] The following set of equations was supplied to the students to help them better understand the reaction:

$$Fe^{3+} + H_2O_2 + e^- \rightarrow Fe^{2+} + OH^- + {}^{\bullet}OH$$

$$Fe^{2+} + H_2O_2 \rightarrow Fe^{3+} + OH^- + {}^{\bullet}OOH$$

$$OH/{}^{\bullet}OOH + \text{dye} \rightarrow H_2O + \text{colorless oxidized dye fragments.}$$

The pseudo-first order kinetic graph in Fig. 8(b) plots the natural logarithm of the absorbance at λ_{max} as a function of time. The students were reminded of Lambert–Beer law, and of the fact that the absorbance of the dye is directly proportional to its concentration in the reaction system. The slope of this plot provided the pseudo-first-order rate constant, k_{app}. Averaging k_{app} from all successful experiments provides an average value of 0.025 min^{-1} with a standard deviation of 0.01 min^{-1}. Table 3 compares our k_{app} values with some other examples of methylene blue degradation catalyzed by IONPs.

4 Conclusions

In this report, we discuss the development and deployment of a multi-week laboratory activity aimed at equipping novice

Open Access Article. Published on 06 2025. Downloaded on 05-12-2025 9:17:44.
This article is licensed under a Creative Commons Attribution-NonCommercial 3.0 Unported Licence.

nanochemistry students with an effective 'methods' toolkit whose components they will revisit repeatedly during the semester-long course. Centered on the synthesis and characterization of iron oxide nanoparticles, this experiment provides an excellent training opportunity, setting students up to engage in a course-based undergraduate research experience. The straightforward synthesis of a relatively benign yet functionally enriched inorganic material – nanosized iron oxide particles capped with CTAB – is followed by an extensive suite of structural and functional characterization protocols, culminating in a simple catalytic application of IONP@CTAB. We contend that this is an eminently suitable replacement for 'piecemeal' or 'cookbook'-style laboratory activities for upper-division UG labs with an inorganic, materials, or nanochemistry focus. The activity is 'green', affordable, and has an unique flexibility of scope in the sense that it is open to a variety of changes through addition or curtailing of secondary characterization protocols. Finally, the proposed activity aligns with the United Nations Sustainable Development Goals (UN SDGs) 4 (Quality Education for All) and 6 (Clean Water and Sanitation). This work represents the first in a series of equitable CUREs that we are developing to enhance the quality of training and laboratory experience for undergraduate chemistry students at Colorado State University.

Data availability

The data supporting this article have been included as part of the ESI,† as well as in the figures and tables of the main article. Raw data generated by the students will be anonymized and produced upon request.

Author contributions

Conceptualization – AB; data curation – AB, TS, BM; formal analysis – AB, TS, BM; funding acquisition – AB; investigation – TS, DM; methodology – AB, BM; project administration – AB; supervision – AB; visualization – AB, BM; writing (original draft) – AB, BM; writing (review & editing) – all authors.

Conflicts of interest

There are no conflicts to declare.

Acknowledgements

We acknowledge the help we received from Analytical Resources Core (ARC; RRID: SCR-021758) scientists (Drs Ethan Crace, Indrani Bhowmick, and Rebecca Miller) for the duration of this experiment. Anton Paar USA is acknowledged for their loan of an evaluation model of the LiteSizer 500 for the duration of the course. The department of chemistry at Colorado State University, Fort Collins, provided the necessary resources for the completion of this study. The TOC figure was created by Brittany Becker, an artist residing in Saskatoon, SK, who specializes in science communication-related illustrations.

Notes and references

1 G. Chen, I. Roy, C. Yang and P. N. Prasad, *Chem. Rev.*, 2016, **116**, 2826–2885.
2 G. Chen, J. Seo, C. Yang and P. N. Prasad, *Chem. Soc. Rev.*, 2013, **42**, 8304–8338.
3 R. Schloegl and S. B. Abd Hamid, *Angew. Chem., Int. Ed.*, 2004, **43**, 1628–1637.
4 M. Sen, *Nanotechnology and the Environment*, InTech Open, London, UK, 2020.
5 B. A. Maher, I. A. Ahmed, V. Karloukovski, D. A. MacLaren, P. G. Foulds, D. Allsop, D. M. Mann, R. Torres-Jardón and L. Calderon-Garciduenas, *Proc. Natl. Acad. Sci.*, 2016, **113**, 10797–10801.
6 P. Mehndiratta, A. Jain, S. Srivastava and N. Gupta, *Environ. Pollut.*, 2013, **2**, 49–58.
7 C. O'Connor and H. Hayden, *Chem. Educ. Res. Pract.*, 2008, **9**, 35–42.
8 M. Pagliaro, *Chem.–Eur. J.*, 2015, **21**, 11931–11936.
9 J. M. Mutambuki, PhD thesis, Mallinson Institute for Science Education, Western Michigan University, Michigan, 2014.
10 M. G. Jones, R. Blonder, G. E. Gardner, V. Albe, M. Falvo and J. Chevrier, *Int. J. Sci. Educ.*, 2013, **35**, 1490–1512.
11 J. M. Mutambuki, H. Fynewever, K. Douglass, W. W. Cobern and S. O. Obare, *J. Chem. Educ.*, 2019, **96**, 1591–1599.
12 J. Schindelin, I. Arganda-Carreras, E. Frise, V. Kaynig, M. Longair, T. Pietzsch, S. Preibisch, C. Rueden, S. Saalfeld and B. Schmid, *Nat Methods*, 2012, **9**, 676.
13 M. Feder and S. Malcom, *Barriers and Opportunities for 2-year and 4-year STEM Degrees: Systemic Change to Support Students' Diverse Pathways*, National Academies Press, 2016.
14 M. C. Linn, E. Palmer, A. Baranger, E. Gerard and E. Stone, *Science*, 2015, **347**, 1261757.
15 J. M. Kevin Eagan, S. Hurtado, M. J. Chang, G. A. Garcia, F. A. Herrera and J. C. Garibay, *Am. J. Educ. Res.*, 2013, **50**, 683–713.
16 L. C. Auchincloss, S. L. Laursen, J. L. Branchaw, K. Eagan, M. Graham, D. I. Hanauer, G. Lawrie, C. M. McLinn, N. Pelaez, S. Rowland, M. Towns, N. M. Trautmann, P. Varma-Nelson, T. J. Weston and E. L. Dolan, *CBE: Life Sci. Educ.*, 2014, **13**, 29–40.
17 K. V. Desai, S. N. Gatson, T. W. Stiles, R. H. Stewart, G. A. Laine and C. M. Quick, *Adv. Physiol. Educ.*, 2008, **32**, 136–141.
18 G. Bangera and S. E. Brownell, *CBE: Life Sci. Educ.*, 2014, **13**, 602–606.
19 F. M. Watts and J.-M. G. Rodriguez, *J. Chem. Educ.*, 2023, **100**, 3261–3275.
20 J. R. Raker, J. M. Pratt, M. C. Connor, S. R. Smith, J. L. Stewart, B. A. Reisner, A. K. Bentley, S. Lin and C. Nataro, *J. Chem. Educ.*, 2022, **99**, 1971–1981.
21 J. R. Raker, B. A. Reisner, S. R. Smith, J. L. Stewart, J. L. Crane, L. Pesterfield and S. G. Sobel, *J. Chem. Educ.*, 2015, **92**, 973–979.
22 J. B. Zimmerman, P. T. Anastas, H. C. Erythropel and W. Leitner, *Science*, 2020, **367**, 397–400.

© 2025 The Author(s). Published by the Royal Society of Chemistry

Open Access Article. Published on 06 2025. Downloaded on 05-12-2025 9:17:44.
This article is licensed under a Creative Commons Attribution-NonCommercial 3.0 Unported Licence.

23 M. L. Landry, T. E. Morrell, T. K. Karagounis, C.-H. Hsia and C.-Y. Wang, *J. Chem. Educ.*, 2014, **91**, 274–279.
24 A. D. Urbina, H. Sridhara, A. Scholtz and A. M. Armani, *J. Chem. Educ.*, 2024, **101**, 2039–2044.
25 A. Banerjee, W. Zeng, M. Taheri, B. Blasiak, B. Tomanek and S. Trudel, *AIP Adv.*, 2019, **9**, 125031.
26 W. Wu, Q. He and C. Jiang, *Nanoscale Res. Lett.*, 2008, **3**, 397–415.
27 T. Zeng, W.-W. Chen, C. M. Cirtiu, A. Moores, G. Song and C.-J. Li, *Green Chem.*, 2010, **12**, 570–573.
28 R. Hudson, A. Riviere, C. M. Cirtiu, K. L. Luska and A. Moores, *Chem. Commun.*, 2012, **48**, 3360–3362.
29 J. Filser, D. Arndt, J. Baumann, M. Geppert, S. Hackmann, E. M. Luther, C. Pade, K. Prenzel, H. Wigger, J. Arning and M. Hohnholt, *Nanoscale*, 2013, **5**, 1034–1046.
30 S. Aula, S. Lakkireddy, A. Kapley, N. Hebalkar, R. K. Sharma, S. G. Uppin and K. Jamil, *Curr. Nanomed.*, 2021, **11**, 70–80.
31 M. D. Nguyen, H.-V. Tran, S. Xu and T. R. Lee, *Appl. Sci.*, 2021, **11**, 1–11.
32 A. Banerjee, B. Blasiak, E. Pasquier, B. Tomanek and S. Trudel, *RSC Adv.*, 2017, 38125–38134.
33 S. Trudel and A. Banerjee, Bi-modal analysis agent, *US Pat.*, 16/515,782, 2020.
34 H.-Y. Lee, S.-H. Lee, C. Xu, J. Xie, J.-H. Lee, B. Wu, A. L. Koh, X. Wang, R. Sinclair, S. X. Wang, D. G. Nishimura, S. Biswal, S. Sun, S. H. Cho and X. Chen, *Nanotechnology*, 2008, **19**, 165101.
35 A. Dash, B. Blasiak, B. Tomanek, A. Banerjee, S. Trudel, P. Latta and F. C. van Veggel, *ACS Appl. Nanomater.*, 2021, **4**, 1235–1242.
36 A. Banerjee, R. Theron and R. W. Scott, *Chem. Commun.*, 2013, **49**, 3227–3229.
37 A. Banerjee, Y. Yao, M.-R. R. Durr, W. G. Barrett, Y. Hu and R. W. Scott, *Catal. Sci. Technol.*, 2018, **8**, 5207–5216.
38 W. Alice, B. Matthias, M. Matthias and A.-J. von Wangelin, *ChemCatChem*, 2012, **4**, 1088–1093.
39 D. S. Chaudhari, R. P. Upadhyay, G. Y. Shinde, M. B. Gawande, J. Filip, R. S. Varma and R. Zboril, *Green Chem.*, 2024, **26**, 7579–7655.
40 S. Hihath, R. A. Kiehl and K. v. Benthem, *J. Appl. Phys.*, 2014, **116**, 1–8.
41 S. Okazoe, Y. Yasaka, M. Kudo, H. Maeno, Y. Murakami and Y. Kimura, *Chem. Commun.*, 2018, **54**, 7834–7837.
42 S. Zhang, Y. Zhang, Y. Wang, S. Liu and Y. Deng, *Phys. Chem. Chem. Phys.*, 2012, **14**, 5132–5138.
43 Y. Yao, C. Patzig, Y. Hu and R. W. J. Scott, *J. Phys. Chem. C*, 2015, **119**, 21209–21218.
44 T. N. Gieshoff, A. Welther, M. T. Kessler, M. H. Prechtl and A. J. von Wangelin, *Chem. Commun.*, 2014, **50**, 2261–2264.
45 M. Jacinto, V. Silva, D. Valladão and R. Souto, *Biotechnol. Lett.*, 2021, **43**, 1–12.
46 A. P. LaGrow, M. O. Besenhard, A. Hodzic, A. Sergides, L. K. Bogart, A. Gavriilidis and N. T. K. Thanh, *Nanoscale*, 2019, **11**, 6620–6628.
47 R. Mori Junior, J. Fien and R. Horne, *Sustain. J. Rec.*, 2019, **12**, 129–133.
48 C. F. Macrae, I. Sovago, S. J. Cottrell, P. T. Galek, P. McCabe, E. Pidcock, M. Platings, G. P. Shields, J. S. Stevens, M. Towler and P. A. Wood, *Appl. Crystallogr.*, 2020, **53**, 226–235.
49 R. Raciti, R. Bahariqushchi, C. Summonte, A. Aydinli, A. Terrasi and S. Mirabella, *J. Appl. Phys.*, 2017, **121**, 1–11.
50 A. J. Deotale and R. Nandedkar, *Mater. Today: Proc.*, 2016, **3**, 2069–2076.
51 J. Klein, L. Kampermann, B. Mockenhaupt, M. Behrens, J. Strunk and G. Bacher, *Adv. Funct. Mater.*, 2023, **33**, 2304523.
52 A. Banerjee, R. Theron and R. W. Scott, *ChemSusChem*, 2012, **5**, 109–116.
53 J. A. Ramos Guivar, E. A. Sanches, C. J. Magon and E. G. Ramos Fernandes, *J. Electroanal. Chem.*, 2015, **755**, 158–166.
54 B. Nikoobakht and M. A. El-Sayed, *Langmuir*, 2001, **17**, 6368–6374.
55 O. Abu-Noqta, A. Aziz and A. Usman, *Mater. Today: Proc.*, 2019, **17**, 1072–1077.
56 F. Stossi and P. K. Singh, *Curr. Protoc.*, 2023, **3**, e849.
57 D. Kumar, H. Singh, S. Jouen, B. Hannoyer and S. Banerjee, *RSC Adv.*, 2015, **5**, 7138–7150.
58 P. Guardia, A. Labarta and X. Batlle, *J. Phys. Chem. C*, 2011, **115**, 390–396.
59 G. McCarthy, J. Holzer, W. Syvinski, K. Martin and R. Garvey, *Adv. X-Ray Anal.*, 1990, **34**, 369–376.
60 G. Carbajal-Franco, E. Rendón-Lara, I. Abundez-Barrera and A. Vásquez-Aguilar, *Mater. Res. Express*, 2020, **7**, 035903.
61 A. Rajan, M. Sharma and N. K. Sahu, *Sci. Rep.*, 2020, **10**, 15045.
62 G. Shi, S. Zeng, Y. Liu, J. Xiang, D. Deng, C. Wu, Q. Teng and H. Yang, *Ecotoxicol. Environ. Saf.*, 2023, **263**, 115240.
63 I. Khan, K. Saeed, I. Zekker, B. Zhang, A. H. Hendi, A. Ahmad, S. Ahmad, N. Zada, H. Ahmad, L. A. Shah, T. Shah and I. Khan, *Water*, 2022, **14**, 242.
64 M. B. Goudjil, H. Dali, S. Zighmi, Z. Mahcene and S. E. Bencheikh, *Desalin. Water Treat.*, 2024, **317**, 100079.
65 H. Wang and Y. Huang, *J. Hazard. Mater.*, 2011, **191**, 163–169.
66 D. Kadhim, A. Muslim and W. M. S. Abid, *Nat. Resour. Hum. Health*, 2023, **3**, 355–363.
67 L. M. Mahlaule-Glory, S. Mapetla, A. Makofane, M. M. Mathipa and N. C. Hintsho-Mbita, *Heliyon*, 2022, **8**, 1–6.
68 S. I. Wanakai, P. G. Kareru, D. S. Makhanu, E. S. Madivoli, E. G. Maina and A. O. Nyabola, *SN Appl. Sci.*, 2019, **1**, 1–10.
69 M. S. Akhtar, S. Fiaz, S. Aslam, S. Chung, A. Ditta, M. A. Irshad, A. M. Al-Mohaimeed, R. Iqbal, W. A. Al-Onazi, M. Rizwan and Y. Nakashima, *Sci. Rep.*, 2024, **14**, 18172.
70 T. de Oliveira Guidolin, N. M. Possolli, M. B. Polla, T. B. Wermuth, T. Franco de Oliveira, S. Eller, O. R. Klegues Montedo, S. Arcaro and M. A. P. Cechinel, *J. Cleaner Prod.*, 2021, **318**, 128556.
71 L. A. da Silva, S. M. S. Borges, P. N. Paulino, M. A. Fraga, S. T. de Oliva, S. G. Marchetti and M. do Carmo Rangel, *Catal. Today*, 2017, **289**, 237–248.
72 R. Noyori, M. Aoki and K. Sato, *Chem. Commun.*, 2003, 1977–1986.
73 R. J. Wydra, C. E. Oliver, K. W. Anderson, T. D. Dziubla and J. Z. Hilt, *RSC Adv.*, 2015, **5**, 18888–18893.